PAPER

Nucleosynthesis in relation to cosmology

To cite this article: Mounib F El Eid 2018 *Phys. Scr.* **93** 044001

IOP Publishing Physica Scripta
Phys. Scr. 93 (2018) 044001 (9pp) https://doi.org/10.1088/1402-4896/aaac69

Nucleosynthesis in relation to cosmology

Mounib F El Eid

American University of Beirut, Department of Physics, Beirut, Lebanon

E-mail: meid@aub.edu.lb

Received 30 June 2017, revised 2 January 2018
Accepted for publication 1 February 2018
Published 7 March 2018

Abstract

While the primordial (or Big Bang) nucleosynthesis delivers important clues about the conditions in the high red-shift universe (termed *far-field cosmology*), the nucleosynthesis of the heavy elements beyond iron by the *r-process* or the *s-process* deliver information about the early phase and history of the Galaxy (termed *near-field cosmology*). In particular, the r-process nucleosynthesis is unique, because it is a primary process that helps to associate individual stars with the composition of the protocloud. The present contribution is intended to give a brief overview about these nucleosynthesis processes and describe their link to the early universe, stellar evolution and to the chemical evolution of the Galaxy. The focus of this present contribution is on illumination the role of nucleosynthesis in the Universe. Owing to the complexity of this subject, a general scenario is more appealing to address interested readers.

Keywords: Nucleosytnthesis, cosmology, early universes, stellar evolution

(Some figures may appear in colour only in the online journal)

1. Introduction

We are lucky to live in what will eventually be the best time in which to explore the mysteries of the Universe. Quoting an interesting sentence in the book by [1], 'We live in a very special time in the evolution of the Universe: the time when we can observationally verify that we live in very special time in the evolution of the Universe'. Imagine that an observer present when the Universe was young would not have been able to know about dark energy, since it had no effect on the expansion rate of the Universe. Observers in the far future will not be able to tell that they live in an expanding universe and would not be able to infer the presence of dark energy either, since all longest lived stars will have ended their evolution. Talking about galaxies, one means *near-field cosmology*, while the high red-shift universe is associated with the *far-field cosmology*. For the reader to get a feeling about high red-shift (z), at a recombination time about 380,000 years after the Big Bang was z = 1100. A review article dealing with this subject is given by [2].

The present paper deals with some aspects of nuclear astrophysics, which is a fundamental part of Astronomy. Imagine that without the helium fusion in red giant stars, the element carbon would not be produced, which is the basic element of our DNA, or a basic element of our existence. The main concern of the present contribution is to describe what the nucleosynthesis of diverse elements and their isotopes reveals about several features of the evolution of the Universe and the Galaxy. In section 2 comments on the primordial nucleosynthesis are presented. In section 3 we deal with the nucleosynthesis of heavy elements beyond iron in stars. Concluding remarks are given in section 4.

2. Primordial nucleosynthesis

2.1. General remarks

The Big Bang nucleosynthesis (BBN) is the first nucleosynthesis process in the Universe to produce elements and their isotopes. Thus, it reveals useful information about the high red-shift universe. The BBN calculations (see reviews by ([3, 31]) assume standard particle physics and a cosmological principle. A cosmological principle assumes that on the large scale at any given time the Universe will be viewed the same from any location. The geometry is described by the Robertson-Walker metric:

$$ds^2 = c^2dt^2 - a^2(t)\left(\frac{dr^2}{1-kr^2} + r^2d\theta^2 + r^2\sin^2\theta d\phi^2\right) \quad (1)$$

The factor k is the curvature term (k = 0 for 3-dim Euclidian flat universe, k = +1 for positively 3-dim space, k = −1 for negatively curved 3-dim space). The scale factor a(t) specifies the adiabatic expansion of the Universe considered to act as a perfect fluid. If a(t) grows with time, the observers see other points in the Universe receding radially, which indicates the *Hubble expansion*. The expansion is described by the Friedmann equation:

$$H^2 = \left(\frac{\dot{a}}{a}\right)^2 = \frac{1}{3}8\pi G\rho - \frac{kc^2}{a^2} + \frac{1}{3}\Lambda \quad (2)$$

where Λ is the cosmological constant. Taking $\Lambda = 0$, the so-called critical density corresponding to k = 0 is given by:

$$\rho_c = \frac{3H_0^2}{8\pi G} = 1.88 \times 10^{-26} h_0^2 \text{ kg.m}^{-3} \quad (3)$$

where $h_0 = H_0/(100 \text{ km/s/Mpc})$ and H_0 is the present Hubble constant. Taking the value of $H_0 = 67.8 \pm 0.9$ Km/Mpc/sec according to the evaluation of the Satellite Planck, [32], $\rho_c = 8.64 \times 10^{-27}$ kg.m^{-3}. For the less informed reader, a present Hubble constant of 70 km /s/Mpc means that if a galaxy is located at 1.0 Mpc (one pc is equal to 3.26 light years, and a light year is 9.46×10^{12} km), then it will be receding at 70 km/s from the solar system

2.2. The deuterium–helium connection

It was always a mystery why the mass fraction (or abundance by mass) of the element helium was always observed higher than about 0.23, since it is not produced in stars at this level. Another question was where the deuterium has been produced, since it is destroyed in stars. The BBN has answered many of these questions and some are still to be answered. The early universe must have been populated with vast numbers of neutrinos (ν) and antineutrinos ($\bar{\nu}$). These particles have very small masses, so that their threshold temperature is low. They are involved in transforming neutrons to protons and vice versa according to the following reactions:

$$\nu_e + n \leftrightarrow p + e^- \quad (4)$$

$$e^+ + n \leftrightarrow p + \bar{\nu_e} \quad (5)$$

$$n \leftrightarrow p + e^- + \bar{\nu}_e. \quad (6)$$

These reactions maintain equilibrium abundances of the neutrons and protons as indicated by the double arrows, which is given by (see [13]) as:

$$\frac{n}{p} = \exp(-\Delta mc^2/kT), \quad (7)$$

where $\Delta mc^2 = 1.293$ Mev is the mass difference between neutrons and protons. This abundance ratio *freezes out* when the time scale of weak interactions becomes larger than the expansion rate given by $(a/\dot{a})$. This occurs when the temperature drops below 10^{10} K when the Universe was about one second old. At that time, the neutron fraction according to equation (7) was

$$\frac{n}{n+p} = 0.21 \quad (8)$$

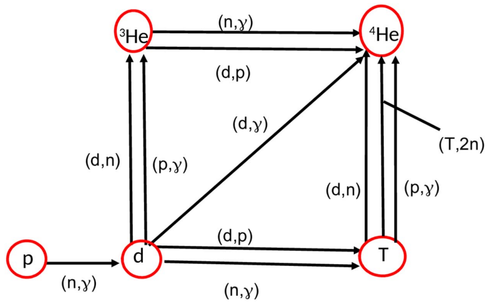

Figure 1. The most important reactions involved in the primordial nucleosynthesis of ^{4}He. The role of deuterium (d) is essential in this process, see text.

where this value depends on the temperature at freeze out. The neutron mass fraction decreased very slowly in the course of time. It can be shown (see [13]) that after 5 min the neutron mass fraction has decreased to 0.123. During this stage, the major production of the light elements took place. Almost all the neutrons were combined with the protons to form ^{4}He nuclei, which means that for every pair of neutrons a helium nucleus was formed. The main reactions involved in producing ^{4}He are shown in figure 1. This figure indicates that deuterium plays a central role in the ^{4}He synthesis. The reactions with deuterium lead to the formation of T and ^{3}He which enable the formation of ^{4}He. Very interesting features are related to the role of deuterium:

- A crucial point is the phenomenon of the so-called deuterium bottleneck, which means that the helium synthesis does not occur until the deuterium achieves a maximum abundance (see figure 3, left panel). As seen in that figure, the abundance of deuterium is negligible, until a temperature $T \leqslant 1.2 \times 10^9$ K is reached. Knowing that the binding energy of deuterium is 2.23 MeV, which corresponds to $T = 2.6 \times 10^{10}$ K, why is it substantially destroyed below this temperature? The reason is due to the number density of the dissociating photons with energies higher than the binding energy of deuterium. It can be shown (see [4]) that the total number density of photons is given by:

$$N_\gamma = 0.244\left(\frac{2\pi kT}{hc}\right)^3 \text{ m}^{-3}. \quad (9)$$

  The dependence of N_γ as a function of temperature is given in figure 2, which indicates strong variation, so that when the temperature drops to $T \leqslant 1.2 \times 10^9$ K (about a factor of 26), the number of the dissociating photons become fewer than the number of nucleons. Clearly, the expansion rate of the Universe plays a crucial role in this process.
- The formation of deuterium is crucial in the BBN. If too much deuterium is produced, then neutrons are locked up and no heavier species will be formed. If little deuterium is produced, then an important factor in the fusion process will be missing, since ^{4}He can form only when deuterium can be formed as explained above. Let us see what we learn from the standard BBN. In figure 3, the resulting

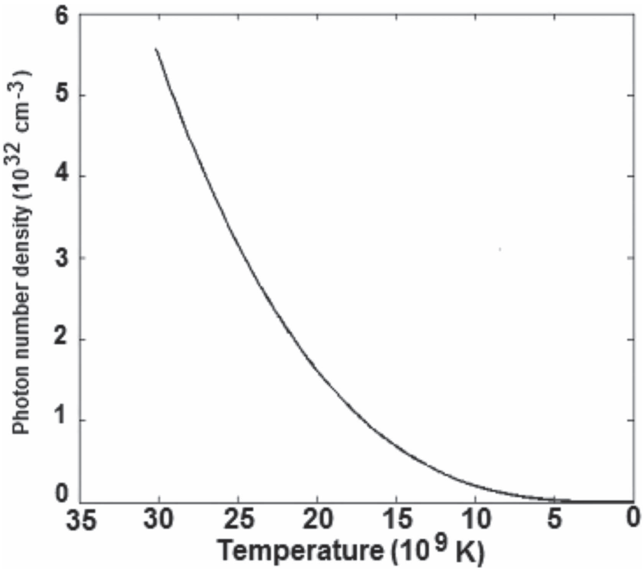

Figure 2. Variation of the photon number density (N_γ) as a function of temperature prior to the onset of Big Bang nucleosynthesis, see text.

mass fractions of the produced species are shown as a function of time and temperature (left panel), while the right panel of that figure shows the abundances as a function of $\Omega_B.h^2$, where Ω_b is the baryon density, $h = H_0/100$ and $H_0 = 69.32$ km/Mpc/s is the present Hubble constant according to the evaluation obtained from the observations using the satellite Planck, [32]. Plenty of features can be learned from these results.

- Only elements up to ^{7}Li are produced. This is because of the fast expansion of the Universe and due to the unstable nuclei with mass numbers A = 5 and 8. In particular, hydrogen is produced at the level of 0.75 by mass fraction, and the mass fraction of ^{4}He lies in the range 0.23–0.25.
- The ^{4}He abundance is nearly constant, since it is fixed through the equilibrium abundance of the neutrons and protons. By contrast with ^{4}He, the other nuclear species are remarkably variable; in particular, deuterium turns out to be very sensitive to the baryon density, and its observed abundance indicates a lower limit of its primordial value, since it is destroyed in stars. Thus, the observed value of $d/H = (2.53 \pm 0.04) \times 10^{-5}$ according to [33], indicates an upper value of the baryon density of $\rho_b = 4.17 \times 10^{-31}$ g/cm^3.

By contrast with deuterium, ^{3}He is created in stars, and can be only observed in an interstellar medium of the Galaxy, which means that its primordial abundance cannot be determined reliably. In other words, it cannot be used as constraints to the BBN ([34].

What is remarkable is the narrow density range (see figure 3) based on the abundances of these two nuclei. It turns out that the present density of the Universe is about 4% of the critical density, so that the baryon density cannot close the Universe and cannot account for dark matter. Also, the comparison with observations as shown in the right panel of figure 3 yields $\Omega_b.h^2 \leqslant 0.015$. This means that even with a low value $h = 0.5$, $\Omega_b = 0.06$ meaning that the baryon density cannot close the Universe and cannot account for dark matter as well. It is emphasized that the results in figure 3 rely on *three neutrino families*. Additional equivalent neutrinos will increase the relativistic degree of freedom and consequently the time-temperature relation, so that the resulting abundances of BBN will be modified (see discussion in [31]).

As seen in figure 3, the predicted abundances of all nuclei match the observation range, except of ^{7}Li which is overproduced in the calculation of BBN (see figure 3, right panel), This finding came out after the physical conditions under which the primordial nucleosynthesis occurred have been constrained by the observations of the fluctuations of the Cosmic Microwave Background. Thus, one faces a *cosmological lithium problem*. This fact and the observed significant variation of the ^{7}Li abundance in very metal-poor stars ([14] need to be resolved. More details concerning this issue are presented in [5].

3. Nucleosynthesis in stars

3.1. General comments

The production of elements and their isotopes in stars is linked to their evolutionary phases and depends on the mass and initial composition of the stars. An overview about the approximate mass ranges is briefly as follows:

- Single stars in the mass range $M = (1\text{–}8)M_\odot$ evolve through the red giant phase and the phase of asymptotic giant branch (briefly: AGB). The AGB phase is characterized by thermal pulsation(see section 3 for some details) leading to heavy mass loss which forms planetary nebulae surrounding a white dwarf. The pulsation of these stars is the site of about half of the heavy element beyond iron in the Galaxy by the so-called *s-process nucleosynthesis*, which is described in section 3.
- Stars of masses $M = (9\text{–}140)M_\odot$ evolve throughout all the evolutionary phases toward core collapse followed by a supernova explosion leading to the formation of neutron stars or black holes. For a long time, the view was that successful supernovae are the major site of about half of the heavy elements beyond iron but including neutron-rich nuclei and super heavy nuclei like uranium and thorium. The r-process nucleosynthesis is responsible for this production of heavy elements (see section 3). However, the discovery of neutron star mergers (NSM) by the LIGO collaboration has drastically changed this picture. The major site of the r-process seems to be the NSM. The role of supernovae explosions in the production of the r-process species seems to be restricted to special and rare events in the early phase of galactic evolution. We give more details in section 3 and mention here the recent review by [39] concerning the NSM.
- Stars of masses above $140\,M_\odot$ develop very massive oxygen cores and could become disrupted by explosive

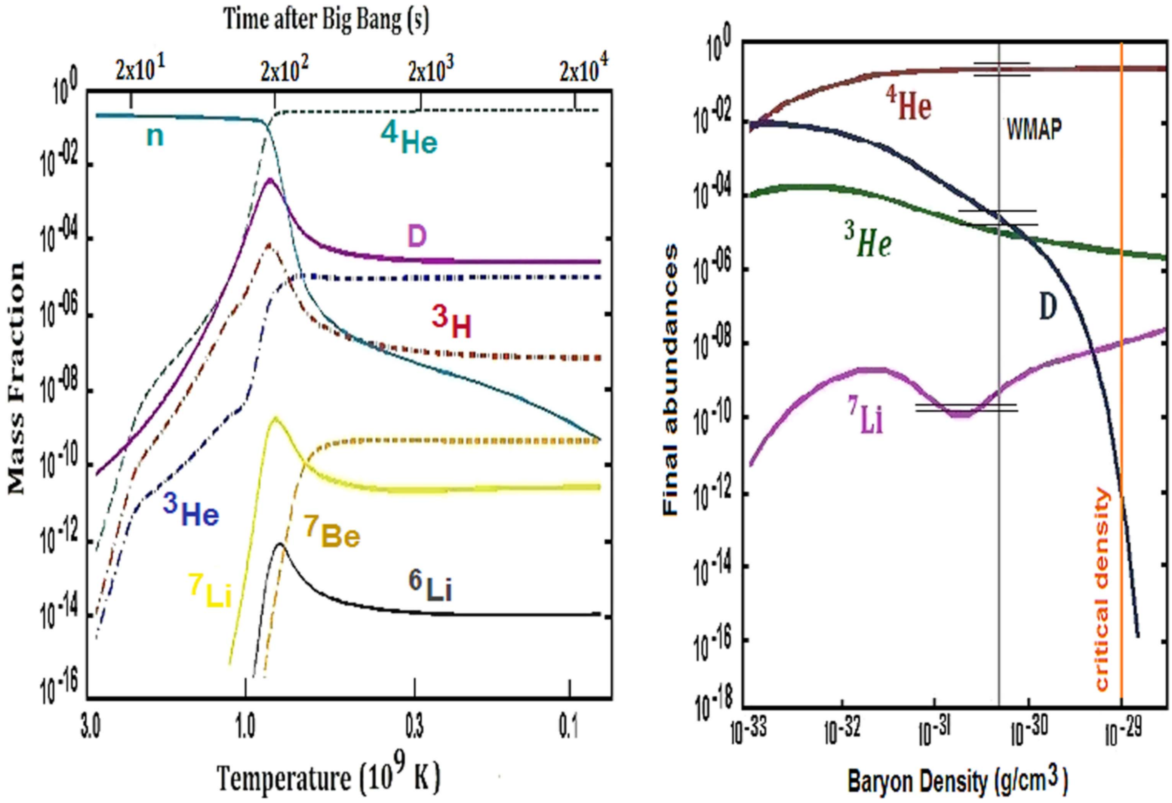

Figure 3. Resulting abundances from Big Bang nucleosynthesis (see [5])) showing the mass fractions of nuclear species up to ^{7}Li as a function of temperature and time. The right panel shows the mass fractions as a function of $\Omega_b.h^2$, where Ω_b is the baryon density and $h = H_0/100$. Comparison with observations, as indicated by the horizontal lines, indicate that ^{7}Li is overproduced, see text.

oxygen burning in a gigantic explosion called *pair creation supernova* (PCSN), (see [6, 7]).

3.2. First stars

It took a relatively long time for the first stars to form in the Universe. This may have occurred after the end of the *dark age*, or 400 million years after the recombination epoch (about 380,000 years after Big Bang). These stars, termed pop III stars, were likely very massive owing to the absence of heavy elements in the early molecular clouds where effective cooling and fragmentation were inhibited (see [8]). The nucleosynthesis in this extinct generation of stars is restricted (see [7]) to nuclei with a proton number $Z \leqslant 30$ (or zinc). Thus heavier nuclei were formed in subsequent generation of stars as we will illustrate in the remaining part of this work.

3.3. Formation of heavy elements

Formation of the heavy elements in the Universe is a fundamental and challenging topic in astrophysics. Basically, due to the Coulomb barrier charge particle reactions are not able to synthesize heavy elements.Thus, neutron capture reactions are mainly responsible for creating the heavy elements in the Universe. There are two main processes responsible for their synthesis: the *s-process* and the *r-process*. A third secondary process, termed *p-process* leads to the formation of proton-rich heavy nuclei, bypassed by the other processes. We will

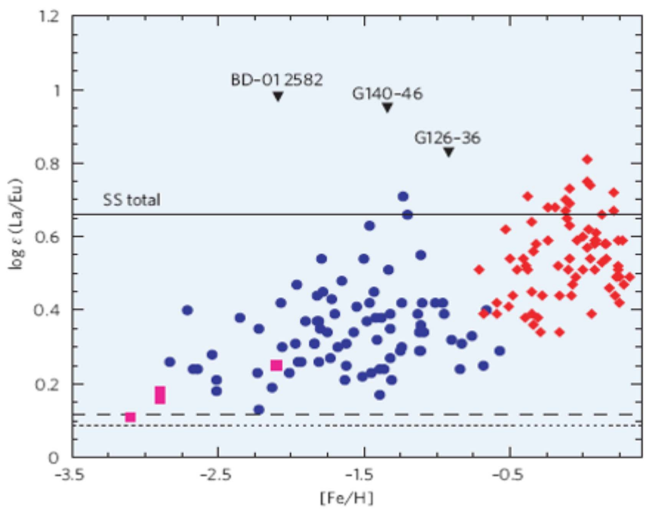

Figure 4. Abundances for the ratio La/Eu versus metallicity for a large number of stars in our Galaxy. Filled circles represent halo stars, filled diamonds are disk stars, and squares represent well-studied r-enhanced stars. Labeled stars are s-process rich. References concerning these data are found in the work by [9] from which this figure is taken. Note that $[Fe/H] = \log(Fe/H)_{star}$-$\log(Fe/H)_{Sun.}$ Adapted from [9].

not describe the p-process in this contribution and refer to the review paper on the r-, s-, and p-processes by [16].

Before describing the s-process and the r-process in some detail, let us explore some information about the galactic evolution of heavy elements. This is indicated in figure 4,

Table 1. Summary of some characteristics of the s-process and r-process.

	s-process	r-process
Neutron density [cm^{-3}]	10^7–10^{11}	10^{20}–10^{30}
Astrophysical site	AGB stars, Massive stars	Supernova type II-Neutron star mergers
Abundances correlated with	Neutron capture cross section	Beta-decay lifetimes
Neutron source	$^{13}C(\alpha, n)^{16}O, ^{22}Ne(\alpha, n)^{25}Mg$	Begin with neutrons & protons
Temperature range	T = (1.5–3.5) × 10^8 K, T ⩾ 10^9 K	T = (1–10) × 10^9 K
Basic characteristic	Secondary process	Primary process

where the abundances for the elemental ratio lanthanum over europium (La/Eu) versus metallicity [Fe/H] is displayed for a large number of stars in our galaxy. The reason for using this ratio is due the fact that La is a main product of the s-process, while Eu is mainly an r-process element. In other words, such a figure helps to identify the astrophysical sites and the timing as a function of metallicity. Figure 4 reveals the following:

(i) The La/Eu ratio increases as the s-process contribution to La rises with metallicity, indicating the role of low mass stars evolving through the AGB phases as mentioned above. These stars are responsible for about half of the heavy elements beyond iron in the Galaxy. Notice that the metal-rich disk stars have a larger ratio than the halo stars, consistent with this picture.

(ii) Figure 4 shows also that only the most metal-poor stars have a La/Eu ratio consistent with the r-process prediction (see dashed line at 0.1 in figure 4). The learned effect is that the r-process seems to have occurred all the time, while the s-process contributed at a later time in the history of the Galaxy, near [Fe/H] = −2.0 and eventually earlier as suggested by [9] and [25]. It seems that more is to learn about the nature of stars and their contribution to the heavy element nucleosynthesis during the early phase of the Galaxy.

It is also instructive to consider the solar system abundance distribution of the r-process and s-process nuclei. As shown in figure 1.2 in [43], which based on the valuation by [42], there are three peaks for both processes with those of the r-processes that are shifted by several units to lower mass numbers, and are broader compared to the peaks of the s-process. These differences are characteristic for these processes. The path of the s-process is close to the valley of stability as it can be seen in figure 9.13 in the text by [26], since the neutron density in the case of the s-process is usually not so high (see table 1) to compete with the β^--decay. As a result the produced peaks along the s-process path are located at the neutron magic numbers: numbers 50, 82 and 126, or at A ≈ 90, 138 and 208. These correspond to elements such as Zr (A ∼ 90), Ba (A ∼ 138), Pb (A ∼ 208). The reason for the occupance of these peaks at the neutron magic numbers is due to the small neutron capture cross section of the magic nuclei.

In case of the r-process, the neutron density is so high with a neutron density in the range 10^{20}–10^{30} cm^{-3}. Consequently, the r-process follows a path far from the valley of stability (see figure 9.13 in the text by [26]). Nuclei with closed neutron shells are still produced abundantly, but they are unstable and undergo β^--decay at constant mass number. For a given magic neutron number, the unstable r-process nuclei have much lower atomic number Z and atomic mass number A than the s-process nuclei. Consequently, the r-process peaks at N = 50,82 and 126 correspond to A ≈ 80, 130 and 195. These correspond to elements such as Kr (A ∼ 85), Xe (A ∼ 130), Pt, Au (A ∼ 195). As the s-process path remains close to the valley of beta stability, only a small range of atomic numbers Z is associated with a closed shell. In case of the r-process, a larger Z-range is involved, which explains the larger width of the r-process peaks. As we see below, the high neutron density involved in the r-process leads to a different flow concept than in case of the s-process.

Another insight comes from observing the r-process rich stars like CS22892-52(see [17]), and the star BD + 17°3248 (see [44]). In figure 5, several features are identified. The heavier n-capture elements of Z ⩾ 56 in the metal poor star CS22892-052 match closely with the solar system r-process distribution. While the solar system s-process does not match the observed data, another remarkable feature in the figure is that the scaled r-process distribution does not extend to the 'light' n-capture elements. This feature is found in many r-process rich stars and cannot be explained by a standard s-process ([17]). It seems that two r-process components are possibly similar to the s-process, but in a context of a more complicated scenario. As outlined below, the core collapse supernovae should be included to explain at least the incomplete r-process.

In figure 14 used in the the work by [12], the abundances of the alpha-element magnesium (^{24}Mg) are compared with those of the element europium (Eu) as a function of metallicity down to [Fe/H] < −3.0. It turns out that the abundances of Mg show very little scatter even at low metallicity. In contrast with Eu showing large scatter at low metallicity (sorry not to show this figure here because of copyright requirement I faced). The interpretation of such observations is (see [22], and references therein) that Mg has been produced significantly in the early phase of the Galaxy by supernova explosions. A remarkable downward decrease of [Mg/Fe] to the solar values indicates the increasing iron production due to its production by type I supernovae.

The data for Eu, which is mainly produced by the r-process nucleosynthesis exhibit large scatter in [Eu/Fe] at low metallicity. This seems to indicate (see [12] and references therein) an early unmixed Galaxy with the supernova events were widely scattered. Moreover the data suggest that

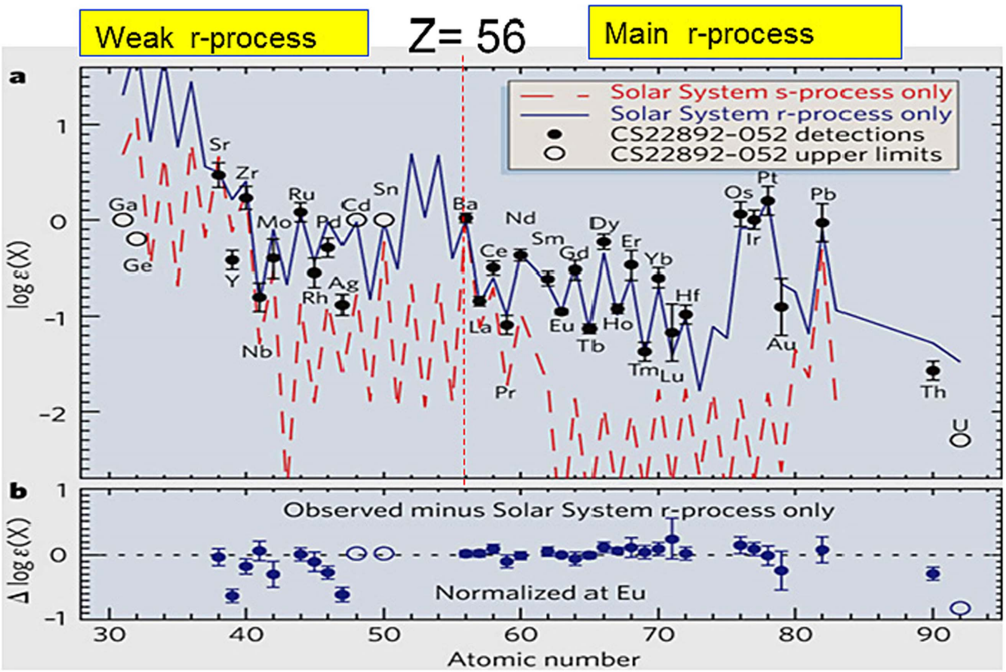

Figure 5. Abundances for the very metal-poor star CS22892-052 according to [18]. This star is r-process rich characterized by [Eu/Fe] $\simeq$ 1.0. Notice that the abundances of heaviest r-process nuclei with Z $\geqslant$ 56 are consistent with the scaled solar r-process abundance distribution, but this is not the case for the lighter nuclei, see text. Adapted from [18].

the r-process production was rare in the early Galaxy. There is also a downward decrease of [Eu/Fe] to the solar value, which is again due to the increasing iron production by type Ia supernovae. On the basis of the above discussion, some implications may be summarized:

- Clear presence of n-capture elements in the atmospheres of metal-poor stars and also globular cluster stars.
- The comparison between r-process rich [Eu/Fe] $\geqslant$ 1.0) and r-process poor ([Eu/Fe] $<$ 1.0) indicates that the abundances of heavy elements with Z $\geqslant$ 56 (Barium and above) are consistent with scaled solar-process distribution. This is now commonly called *main r-process*. However, the distribution of the lighter n-capture elements does not match the solar system pattern. This is now termed *weak r-process*. It seems more convenient to call this component *incomplete r-process*, because the neutron density was not high enough ($<10^{20}$ neutrons/cm^3 (according to [23, 37]) to produce r-process elements beyond the first peak, or Sr region. However, it is emphasized that besides the neutron density the neutron/seed ratio should play a role (see [41]).

3.4. Basic concept of the s-process and the r-process

A comparison between the s-process and the r-process is given in table 1. The temperature range $(1.5 - 3.5) \times 10^8$ K is needed in core helium burning in massive stars (M $\geqslant$ 15 M$_\odot$), or in AGB stars, while T $\geqslant 10^9$ K is needed during shell carbon-burning in massive stars. The temperature range for the r-process is higher whether in neutron star mergers, or in an exploding supernova, where it start near the edge of the newly formed neutron star. In this scenario, the iron-group elements are synthesized *in situ* as explained below.

Regarding the neutron sources, those for the s-process are: $^{13}C(\alpha,\ n)^{16}O$ in AGB stars, while $^{22}Ne(\alpha,\ n)^{25}Mg$ becomes effective in massive stars, and could be activated in massive AGB stars (see [10] concerning this point).

3.5. Comments on the s-process

The s-process is a flow concept process driven by slow neutron capture reactions with relatively low neutron density about $10^7 - 10^{11}$ neutrons/cm^3. Whenever neutrons are produced in stellar environment, they become very quickly (in about 10^{-11} sec) thermalize via s-wave scattering, so that they are described by the Maxwell-Boltzmann distribution (MBD). As mentioned above, the s-process path in the Z-N diagram stays close to the valley of beta-stability in contrast with the r-process path far from the valley of beta-stability. To explain this feature, we use the simplified figure 6. Along the s-process path, the (n,γ) reaction increases the mass number A, but if the isotope is unstable, then the subsequent process depends on the neutron flux (or neutron density) and the β^- half-life time τ_β compared to the neutron capture lifetime, $\tau_{n\gamma}$. In the standard s-process: $\tau_\beta \ll \tau_{n\gamma}$, meaning that beta-decay dominates the flow. Hence, one can follow the change of the number density with time along an isobar (constant mass number A):

$$\frac{dN_A}{dt} = N_n(t)N_{A-1}(t)\langle\sigma v\rangle_{A-1} - N_n(t)N_A(t)\langle\sigma v\rangle_A - N_A\lambda_\beta(t). \quad (10)$$

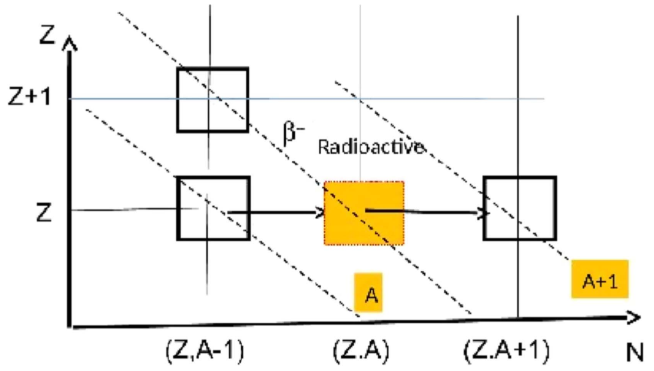

Figure 6. Basic reactions along the s-process path which serve to explain the main characteristics of the s-process as explained in the text.

The first term in equation (10) is a creation term due to the neutron capture, the second term is a destruction term due to further neutron capture, while the third term is destruction by β-decay if it is applicable. Note that the beta decay rate is given by $\lambda_\beta = \frac{ln2}{T_{1/2}(t)}$ and is time dependent in the stellar plasma. Usually, the neutron capture cross section $\sigma_{n\gamma}$ is averaged over the MBD, but in the case of the s-process, the cross section is known experimentally to vary inversely proportional to the velocity of neutrons, $\sigma_{n\gamma} \propto 1/v_n$, or $\propto 1/\sqrt{E_n}$ or $\sigma_{n\gamma} v_n =$ constant. Since the temperature does not vary fast during the s-process, it is convenient to use the neutron thermal velocity $v_T = \sqrt{2kT/m}$. Then, one uses the relation $\langle \sigma v \rangle_{n\gamma} = \langle \sigma \rangle v_T$. Note that $\langle \sigma \rangle$ should be folded with the MBD, but in the case under consideration, $\langle \sigma \rangle = \sigma_T$ that is the cross section at $v = v_T$. A measurement of the cross section near the thermal velocity provides a good value for $\langle \sigma \rangle$.

Back to equation (10), it can be rewritten in more convenient way (see more details in the text by [26]) in the following form:

$$\frac{dN_A}{dt} = v_T N_n(t)(\langle \sigma \rangle_{A-1} N_{A-1} - \langle \sigma \rangle_A N_A). \tag{11}$$

This equation is derived under the assumptions: (i) $\tau_\beta \ll \tau_{n\gamma}$ meaning that radioactive nuclei decay very fast, so that their abundances can be neglected, (ii) $\tau_\beta \gg \tau_{n\gamma}$ meaning that the radioactive nuclei can be treated as stable, (iii) slow variation of temperature during the s-process. Note that the last assumption led to the definition of $\langle \sigma \rangle$ as above. Finally, introducing the neutron flux $\Phi_n(t) = v_T N_n(t)$, the so-called neutron exposure is the given by:

$$\tau = \int_0^t \phi_n(t) dt = v_T \int_0^t N_n(t) dt. \tag{12}$$

With τ as a new variable, equation (11) becomes a very useful equation:

$$\frac{dN_A}{d\tau} = \langle \sigma \rangle_{A-1} N_{A-1} - \langle \sigma \rangle_A N_A. \tag{13}$$

This equation is a self-regulating equation with a steady state solution $\sigma_A N_A = \sigma_{A-1} N_{A-1}$. An illustration of the feature can be seen in figure 9.9 in the text by [26], or in figure 15 in the work by [44]. In those figures, the σ N = constant behavior is clearly seen with a drop at the magic neutron numbers N = 50,82 and 126, where σ is small. This curve shows how the s-process is linked to stellar evolution. The s-process nuclei below A = 90 are produced by the *weak component* of the s-process in massive stars, while the bulk of these s-process nuclei is associated with the *main component* in AGB stars during their thermal pulsations. A review article on this subject is found by [27]. The main advantage of the σ *N*-curve is that it helps to determine the r-process abundances in the Sun. The fact that the this curve is not explaining the data for mass number below A = 90 led to the insight that two components are involved in the s-process as mentioned above.

3.6. Comments on the r-process

The r-process is also based on a flow concept like the s-process (a review article is given by [11]. However, it is a primary process in the Galaxy since it creates its own seed nuclei comprising the iron group nuclei. The basic feature of this process is the extremely high neutron density, in the range $10^{20}-10^{30}$ neutrons/cm^3. Consequently, the lifetime of neutron capture is very short compared to beta-decay lifetime, or $\tau_{n\gamma} \ll \tau_\beta$. As a consequence, neutron capture reactions dominate the flow but not all the time. Due to the fast addition of neutrons, neutron-rich nuclei are formed far from the valley of beta-stability. The beta-decay lifetimes of neutron-rich isotopes are short millisecond to second. Then for $\tau_{n\gamma} \leqslant 1.0$ ms, the neutron density will be $>10^{19}$cm^{-3}. As the neutron number density increases, the neutron binding energy Q_n decreases which tends to approach zero, or neutron drip line. For a given temperature T and neutron density N_n, an equilibrium between the (n, γ)-(γ, n) reaction rates is established, which is described (see [26]) by:

$$\lambda_{\gamma n} \propto (T^{3/2}/N_n) \exp^{-Q_n/KT} \lambda_{n\gamma}. \tag{14}$$

For example, if $N_n = 10^{24}$ cm^{-3} and $T = 10^9$, then $Q_n = 2$ MeV and both rates are equal, so that the (n, γ) chain stops and beta-decay becomes effective. This is called *waiting points* for each charge Z (or isotopes chain). This behavior is clearly seen in figure 9.13 in the text by [26]. This means that the abundances are correlated to N_Z rather than N_A as in the case of the s-process.

In particular, the nucleus ^{130}Cd with its magic N = 82 represents a special *waiting point* for the r-process. The update value of its β^- lifetime is as follows:(127 ± 2)ms according to the RIKEN-results [35], (126 ± 4) ms according to [36]. In other words, the abundances in the r-process are correlated with beta-decay life times while those due to the s-process are correlated with the neutron capture cross section.

3.7. Stellar sites for the s-process and r-process

- **s-process**

As outlined above, the astrophysical aspects of the canonical s-process are that it starts later in the Galaxy, because it is a secondary process requiring iron seed nuclei. The analysis of the curve σ N = constant by [42] led to the insight that two components are needed for the s-process, a *weak component* and a *main component*. The stellar cite of the weak component are the massive stars of masses $M \geqslant 15\, M_\odot$ during their core He-burning phases and shell-carbon burning phases (see [20]), where only the nuclei with mass number $A < 90$ are produced during these phases, and these can be ejected into the interstellar medium by type II supernovae (see remarks in [20]).

The main component leads to the production of Heavier s-process nuclei during the AGB phases of low and intermediate mass stars $(1\text{–}8)M_\odot$ with the main contribution from the range $(1\text{–}3)M_\odot$ (see [27]). Careful modeling of the thermally pulsating AGB stars is required, in particular the production of the main neutron source $^{13}C(\alpha, n)^{16}O$ is highly dependent on the mixing of protons from the convective envelope into the helium and carbon rich layers. A useful review on general properties of AGB stars is given by [10].

The basic structure of an AGB star is illustrated in figure 3 in the review by [10] during two successive thermal pulses. While such a figure is rather illustrative, the modeling of the thermal pulsation is an involved task. A pulse is initiated by the energy flux released by the triple-alpha process, which leads to a violent expansion of the envelope. The convective envelope recedes and the hydrogen burning shell becomes temporally extinct. Due to the expansion, the opacity increases, so that after the pulse ends the envelope convection penetrates into the helium and carbon-rich layers. This is the so-called *third dredge up* (TDUP). This process is required in order to mix processed material to the surface. The s-process nucleosynthesis operates mainly during the inter-pulse period where the neutron source is delivered mainly by the $^{13}C(\alpha, n)^{16}O$ reaction. A basic problem is how to obtain sufficient amount of ^{13}C that can release enough neutrons to match the solar s-process abundance distribution belonging to the main component. The formation of ^{13}C needs extra diffusion of protons into the carbon-rich region (see figure 3 in [10]), a process which is not fully controlled. The investigation by [24] suggests an amount of $4 \times 10^{-3}\, M_\odot$ to explain the s-process abundances in the Galaxy. This work emphasizes an important point that the understanding of s-process should not be restricted to matching the solar s-process abundances but should concern the chemical evolution in the Galaxy. These authors addressed the role of the magnetic field in affecting the amount of ^{13}C.

• **r-process**

Until recently, the most favored cite of the r-process was the high entropy wind (HEW) in core collapse supernova (CCSN). The basic scenario (see, [28, 29]) is that the streaming out neutrinos from the forming neutron star represent a neutrino-driven wind starting near the surface of the newly forming neutron star with a flow of neutrons and protons. In a temperature range $T = (6\text{–}10) \times 10^9$ K, the neutrons and protons combine to form alpha-particles, but with an excess of neutrons. When the temperature drops to the range $T = (3\text{–}6)\times 10^9$ K, nuclei in the iron group are able to form, which serve as seed nuclei for the r-process. This is called *alpha freeze out*. Upon further cooling to the range $T = (1\text{–}3) \times 10^9$ K, the r-process becomes effective.

However, the role of neutron star mergers proposed as a cite of the r-process did not receive enough attention until the recent discovery by the LIGO-collaboration of neutron star merging. The whole picture concerning the cite of the r-process has radically changed. A recent review is given by [38] and the many references therein. It seems clear that neutron star mergers constitute the major cite of the heavy element production by the r-process, and the only source of elements beyond lead and bismuth [38]. The remarkable insight was that the neutron star mergers were identified with a short duration of gamma-ray bursts via their IR afterglow, to be explained by the opacities of heavy elements beyond the iron group.

Does this discussion mean that the core collapse supernovae (CCSN) are removed from being the site of any r-process?. An answer to this question is not straightforward. For example, the behavior of [Eu/Fe] shown in figure 14 in the work by [12] with its large scatter at low metallicities may reveal the role of early CCSN of massive stars. It seems that the large scatter of [Eu/Fe] indicates production with low event rate with high amount of r-process to explain the solar abundance, and a lack of mixing into the interstellar medium of these products steaming from CCSN. In short, the role of CCSN contributing to the r-process cannot be excluded especially at low metallicities. The work presented by [39] suggests a *magnetorotational core collapse supernovae*. They argue for the occurrence of the r-process depending on the strength of the magnetic field, which they assumed to be 10^{11} Gauss, or 10^{12} Gauss. While such calculations suggest this type of supernovae as an r-process site, the origin of the assumed magnetic fields still does not explain the arguement themselves.

It is interesting to mention recent observations of the supernova remnant *Cassiopeia A* by the *NuSTAR* team ([30]), which enabled them to construct a map of the radioactive element ^{44}Ti, which is produced in incomplete silicon-burning near the boundary between the material falling back on the neutron star and the ejected layers. This observation indicates how asymmetric the explosion was. The recent work by [40] compared a 3D simulation of a neutrino-driven explosion of a star of initial mass of a $15\, M_\odot$ with the the observed ^{44}Ti distribution in Cassiopeia A. Their main conclusions are the observed asymmetry, which can be explained by a neutrino-driven explosion, and that the high ^{44}Ti abundance may be explained without rapid rotation or jet-driven explosion. Unfortunately, this work did not address any r-processes in the model computation.

What is important is the r-process signature in halo stars. These stars are the oldest in the Galaxy, therefore they provide important insight about their early production. A well-studied halo star is *CS22892-052* by [12] having [Fe/H] = −3.0. A striking finding is the agreement between the abundances of this star and the solar r-process abundances for $Z \geqslant 56$ (that is starting Ba). However no agreement for range $Z = 40\text{–}50$ (first r-process peak) was found. It is beyond the scope of this contribution to discuss this issue. It seems that the r-process was not happening the same way all the time as it has been thought. There is an incomplete (or weak) component similar to the s-process. More work is needed to understand the nature site of this component.

4. Concluding remarks

A summary of this contribution is as follows:

- The primordial nucleosynthesis is restricted to the light elements up ^{7}Li, but it delivers important clues about the high red-shift universe.
- The early generation of stars (pop III) are not the site of the heavy element production beyond iron.
- The heavy elements and their isotopes are mainly produced by the s-process and the r-process and to less extent by the p-process. They trace back the chemical evolution of the Galaxy, thus they represent a link to the low red-shift universe. Many details of these processes are still not understood, especially the physical conditions under which they operate. In case of the s-process the treatment of mixing on the AGB phase is rather challenging and needs further elaboration; eventually three dimensional simulation is desired to at least test the one-dimensional description. In case of the r-process occurring in core collapse supernovae, the modeling of the explosion is still challenging, especially in light of the newest observations of the radioactive element ^{44}Ti in the supernova remnant *Cassiopeia A* as mentioned above. The site of the r-process has received a new insight after the discovery of neuron star mergers by the the LIGO collaboration.

Acknowledgments

The author thanks an anonymous referee for their help to improve the content. He regrets not being able to display several widely known figures due to copyright requirements.

References

[1] Morison I 2009 *Introduction to Astronomy and Cosmology* (Chicester: Wiley)
[2] Freeman K and Bland-Hawthorn J 2002 *Ann. Rev. A&A* **40** 487
[3] Schramm D and Turner M 1998 *Rev. Mod. Physics* **79** 303
[4] Longair M 2003 *Theretical Concepts in Physics* (Cambridge: Cambridge University Press)
[5] Makki T and El Eid M 2017 *J. Phys. Conf. Ser.* **869** 012091
[6] Ober W, El Eid M and Fricke C 1983 *A&A* **119** 61
[7] Heger A and Woosley S E 2002 *APJ* **567** 532
[8] Bromm V *et al* 2009 *Nature* **459** 29
[9] Simmerer J *et al* 2004 *APJ* **617** 1091
[10] Herwig F 2005 *Ann. Rev. A&A* **43** 435
[11] Cowan J J and Thielemann F-K 2004 *Phys. Today* **47**
[12] Sneden C, Cowan J J and Gallino R 2008 *Ann. Rev. A&A* **46** 241
[13] Weinberg S 1972 *Gravitatiuon and Cosmology* (New York: Wiley)
[14] Sbordone L *et al* 2010 *A&A* **522A** 26S
[15] Tadafumi M *et al* 2017 *Astronomical Society of Japan* **69** 24 arXiv:1612.06624V1 [asto-ph.SR]
[16] Mayer B S 1994 *Ann. Rev. A&A* **32** 152
[17] Cowan J J and Sneden C 2006 *Nature* **440** 1151
[18] Sneden C *et al* 2003 *ApJ* **591** 936
[19] Sneden C *et al* 2009 *ApJS* **182** 80
[20] The L-S, El Eid M F and Meyer B S 2007 *ApJ* **655** 1058
[21] El Eid M F, The L-S and Meyer B S 2009 *Space. Sci. Rev.* **147** 1
[22] Thielemann F-K *et al* 2000 *Mem. Soc. Aston. Ital.* **71** 481
[23] Kratz K L *et al* 2007 *ApJ* **662** 39
[24] Tripella O *et al* 2014 *ApJ* **787** 41
[25] Burris D *et al* 2000 *ApJ* **544** 302
[26] Rolfs C and Rodney W 1988 *Cauldrons in the Cosmos* (Chicago, IL: Chicago University Press)
[27] Busso M *et al* 1999 *Ann. Rev. A&A* **37** 239
[28] Kratz K L 2015 *AIP Cof. Proc.* **1065** 109
[29] Woosley S and Janka T 2005 *Nature Phys* **1** 147
[30] Grefenstette R W *et al* 2014 *Nature* **506** 339
[31] Cyburt R H *et al* 2016 *Rev. Mod. Phys.* **88** 15004
[32] Ade A R *et al* 2016 *Astron. Astrophys.* **594** A13
[33] Gooke R J *et al* 2014 *ApJ* **781** 31
[34] Field B 2011 *Ann. Rev. Part. Scien.* **61** 47
[35] Lorusso G *et al* 2015 *Phys. Rev. Lett.* **114** 192501
[36] Dunlop R *et al* 2016 *Phys. Rev.* C **93** 0628017
[37] Farouky F *et al* 2010 *APJ* **712** 1359
[38] Thielemann F K *et al* 2017 *Ann. Rev. Nucl. Part. Sci.* **67** 253
[39] Nishimura N *et al* 2015 *APJ* **810** 109
[40] Wongwathanarat A *et al* 2017 *APJ* **842** 13
[41] Banerjee P *et al* 2011 *Phys. Rev. Lett.* **106** 201104
[42] Käppeler *et al* 1989 *Carnegie Observatories Astrophysics Series* **52** 945
[43] Cowan J J and Sneden C 2003 *Carnegie Observatories Astrophysical Series* vol 4 origin and evolution of the elements, arXiv:astro-ph/0309802v1
[44] Cowan J J *et al* 2011 *Rev. Mod. Phys.* **69** 996